Local versus basin-scale limitation of marine nitrogen fixation

Thomas Weber[a,1,2] and Curtis Deutsch[a,1]

[a]Department of Atmospheric and Oceanic Science, University of California, Los Angeles, CA 90095

Edited by David M. Karl, University of Hawaii, Honolulu, HI, and approved April 17, 2014 (received for review September 12, 2013)

Nitrogen (N) fixation by diazotrophic plankton is the primary source of this crucial nutrient to the ocean, but the factors limiting its rate and distribution are controversial. According to one view, the ecological niche of diazotrophs is primarily controlled by the ocean through internally generated N deficits that suppress the growth of their competitors. A second view posits an overriding limit from the atmosphere, which restricts diazotrophs to regions where dust deposition satisfies their high iron (Fe) requirement, thus separating N sources from sinks at a global scale. Here we use multiple geochemical signatures of N_2 fixation to show that the Fe limitation of diazotrophs is strong enough to modulate the regional distribution of N_2 fixation within ocean basins—particularly the Fe-poor Pacific—but not strong enough to influence its partition between basins, which is instead governed by rates of N loss. This scale-dependent limitation of N_2 fixation reconciles local observations of Fe stress in diazotroph communities with an inferred spatial coupling of N sources and sinks. Within this regime of intermediate Fe control, the oceanic N reservoir would respond only weakly to enhanced dust fluxes during glacial climates, but strongly to the reduced fluxes hypothesized under anthropogenic climate warming.

Biological N_2 fixation replenishes the oceanic N reservoir, which is continually depleted by bacterial denitrification, maintaining the productivity of the ocean and its biological storage of carbon. The growth of N_2-fixing phytoplankton is influenced by myriad environmental conditions (1), but two are considered most important. First, a deficit of nitrate (NO_3^-) in upwelling deep water is thought to favor diazotrophs by inhibiting their faster-growing competitors, who leave behind residual phosphate (PO_4^{3-}) (2, 3). Second, an abundant supply of trace metals—particularly Fe—that form cofactors to the nitrogenase enzyme is thought to be critical in sustaining rates of N_2 fixation (4). These two sensitivities are not mutually exclusive, but the relative importance of Fe versus N deficits in the ecological niche of diazotrophs leads to distinctly different predictions for both the spatial pattern of N_2 fixation and its response to changes in climate (5).

If a scarcity of NO_3^- is sufficient to ensure favorable conditions for diazaotroph growth, then N_2 fixation should be concentrated in the Pacific Ocean (6), where recently denitrified waters upwell to the surface bearing the largest NO_3^- deficits. In the absence of other limiting factors, N_2 fixation would compensate the N losses close to their origin, and would change in step with denitrification rates but not respond to changing Fe deposition. In contrast, a strong Fe dependence would produce larger N_2 fixation rates in the Atlantic and Indian basins, where windblown dust provides a major conduit for Fe into the upper ocean (7, 8). In this case, diazotroph growth would respond slowly to climatic fluctuations of denitrification in the distant anoxic zones of the Pacific, allowing more persistent imbalances in the N budget and larger fluctuations in the N reservoir (9). Furthermore, cool, dustier climate regimes would promote N_2 fixation and carbon storage, initiating a positive feedback on global climate that provides a potential driving mechanism for Pleistocene glacial–interglacial transitions (4, 10, 11). This Fe-centric view is supported by the abundance of the important diazotroph *Trichodesmium* in the tropical Atlantic Ocean (9, 12), and the global maximum of "excess" NO_3^- observed in the underlying thermocline that has been attributed to remineralization of N-rich diazotrophs (13).

Direct observations of N_2 fixation rates are still too sparse to determine the relative importance of these factors, especially in light of systematic underestimates (14) particularly in unicellular cyanobacteria that dominate the diazotrophic community in the Pacific (15, 16). While observations support a role for both Fe inputs and N losses in regulating marine N_2 fixation (9, 17), the temporal and spatial scales at which they are expressed are poorly understood.

We used an ocean model combined with observed geochemical quantities to constrain the relative influence of Fe and N deficits on rates and patterns of N_2 fixation (see *Materials and Methods*, *SI Materials and Methods*, and Table S1). Modeled cycles of P, N, and Fe are coupled through a simple planktonic ecosystem (18) embedded in a dynamically and observationally constrained ocean General Circulation Model (19). Nutrients are assimilated by two groups of phytoplankton: nondiazotrophic plankton with elemental requirements defined by the ratios R_O (N:P) and Q_O (Fe:P), and diazotrophs that assimilate P and Fe in the ratio Q_F (Fe:P) and introduce new NO_3^- fixed from N_2. The growth rate of nondiazotrophic plankton is reduced when N is scarce, a condition arising from denitrification in anoxic waters and sediments. The rates and distributions of denitrification are prescribed using tracer-based estimates and their uncertainties from inverse models (Fig. S1) (20, 21). This minimizes the errors in geochemical tracer distributions influenced by N loss, allowing those data to constrain N_2 fixation. Diazotroph growth is not susceptible to N limitation but depends on the supply of Fe (both from the atmosphere and deep ocean) per unit of P. The Fe supply is predicted in a model that includes deposition, complexation, and scavenging (22), and reproduces observed patterns of Fe (Fig. S2). Distributions of N_2 fixation and associated

Significance

This paper addresses a longstanding debate regarding the factors that limit nitrogen fixation by diazotrophic plankton—the primary source of an essential nutrient to the ocean. Multiple lines of evidence show that diazotroph growth can be locally limited by the atmospheric iron supply, but large-scale rates of N_2 fixation are ultimately controlled by N deficits generated within the ocean. These findings can reconcile the conflicting observations of biologists and geochemists, while implying a new sensitivity of the marine N cycle to anthropogenic climate warming.

Author contributions: T.W. and C.D. designed research; T.W. performed research; T.W. analyzed data; and T.W. and C.D. wrote the paper.

The authors declare no conflict of interest.

This article is a PNAS Direct Submission.

Freely available online through the PNAS open access option.

[1]Present address: School of Oceanography, University of Washington, Seattle, WA 98195.

[2]To whom correspondence should be addressed. E-mail: tsweber@uw.edu.

This article contains supporting information online at www.pnas.org/lookup/suppl/doi:10.1073/pnas.1317193111/-/DCSupplemental.

geochemical tracers are analyzed after the model N and Fe budgets have reached a close balance.

We manipulated the strength of Fe limitation of model diazotrophs by varying their Fe quota (Q_F) over the interval $1 \leq Q_F/Q_O \leq 50$ (Q_O is constant), which brackets most laboratory observations (see refs. 23–25). The changing patterns of N_2 fixation produced by raising Q_F/Q_O reveal three distinct Fe limitation regimes (Fig. 1). When diazotrophs have similar Fe requirements to other phytoplankton ($Q_F/Q_O < 5$, regime 1), they grow successfully in any region with N deficits strong enough to overcome their slower intrinsic growth rate. N_2 fixation is concentrated where denitrified waters are brought to the surface and first reach oligotrophic habitats, and its partition between ocean basins closely resembles that of denitrification, with the Pacific contributing ~60%. Within the Pacific, N_2 fixation is focused toward the eastern and equatorial gyre margins, where strongly N-deficient waters upwell from suboxic zones (Fig. 1 and Fig. S3*A*).

As the Fe requirement for diazotrophs rises ($5 \leq Q_F/Q_O \leq 25$; regime 2), the distribution of N_2 fixation within the Pacific Ocean undergoes major reorganization. Diazotrophs are displaced from the Fe-poor eastern margin, and relocated westward within the subtropical gyres, where they are better fueled by dust from the East Asian and Australian continents. The proportion of total Pacific N_2 fixation found east of 160°W decreases from ~70% to ~40% over this regime, but the basin-scale rates remain relatively constant (Fig. 1 and Fig. S3*B*). At even higher Fe quotas ($Q_F/Q_O > 25$, regime 3), the Fe demand of diazotrophs cannot be met in the western Pacific either, and N_2 fixation shifts out of the Pacific basin and into the Indian and tropical Atlantic oceans where Fe is more abundant. Its interbasin partition diverges from that of N losses and begins to resemble the distribution of atmospheric Fe inputs as Q_F/Q_O approaches 50 (Fig. 1 and Fig. S3*C*).

The large-scale shifts in diazotrophic habitat induced by varying Fe limitation are associated with detectable changes in several geochemical quantities. These predictions can be tested against established data to determine the regime in which the modern ocean lies.

The most direct diagnostic of a basin-wide rate of N_2 fixation is the degree to which it compensates basin-scale N losses. Under the weak to intermediate Fe limitation of regimes 1 and 2, N_2 fixation is able to closely balance denitrification to within ±5 TgN/y in the Fe-poor Pacific Ocean (Fig. 2*A*). In response to the strong Fe limitation of regime 3, N_2 fixation in the basin falls short of denitrification, with imbalances exceeding 20 TgN/y at $Q_F/Q_O > 30$ and approaching 50 TgN/y in the most Fe-limited scenarios. The difference between biological sources and sinks of N is balanced by a net export of N-deficient water from the basin, closing the Pacific N budget (Fig. 2*A*). The transport of a nitrate deficit into or out of the Pacific Ocean can be directly constrained from observations by estimating the physical convergence of observed $N^* (N^* = [NO_3^-] - 16[PO_4^{3-}])$ across its boundaries (26) in an ocean circulation model, while propagating uncertainties in the nutrient observations. A suite of 10,000 Monte Carlo calculations yields a transport convergence of just 1.3 ± 14.7 TgN*/y into the Pacific, indicating a close balance between denitrification and N_2 fixation in the basin. This value is consistent across three data-constrained circulation models (Fig. S4), and is compatible only with the low and intermediate Fe limitation regimes (Fig. 2*A*).

N_2 fixation leaves well-known regional signatures in the nutrient stoichiometry of the surface ocean, where diazotroph growth consumes excess PO_4^{3-} (or $P^* = [PO_4^{3-}] - [NO_3^-]/16$) (6), and in the underlying thermocline, where the remineralization of their N-rich organic matter (27) releases an excess of NO_3^- relative to PO_4^{3-} (N^*) (13). Both quantities reveal striking differences between a Fe-rich basin with little denitrification (North Atlantic), and a Fe-poor basin with large denitrification zones (North Pacific, Fig. S5). For a given denitrification rate, these tracer differences predominantly reflect the spatially and temporally integrated rates of N_2 fixation, making them a strong constraint on its distribution.

When N_2 fixation is weakly constrained by Fe (regime 1), excess PO_4^{3-} is fully consumed by diazotrophs in all oligotrophic waters, so simulated surface P^* is close to zero in both the North Atlantic and North Pacific Subtropical Gyres (NASG and NPSG, respectively). Its mean difference between gyres ($\Delta P^* = P^*_{NPSG} - P^*_{NASG}$; see *SI Materials and Methods* for gyre definitions) is ~0 μM, lower than the observed value of 0.09 ± 0.04 μM (Fig. 2*B*) computed from a monthly nutrient climatology (28). As Q_F/Q_O increases through regime 2, P^* begins to accumulate in the eastern NPSG, fueling diazotroph growth downstream in the central and western gyre. Its basin-scale difference

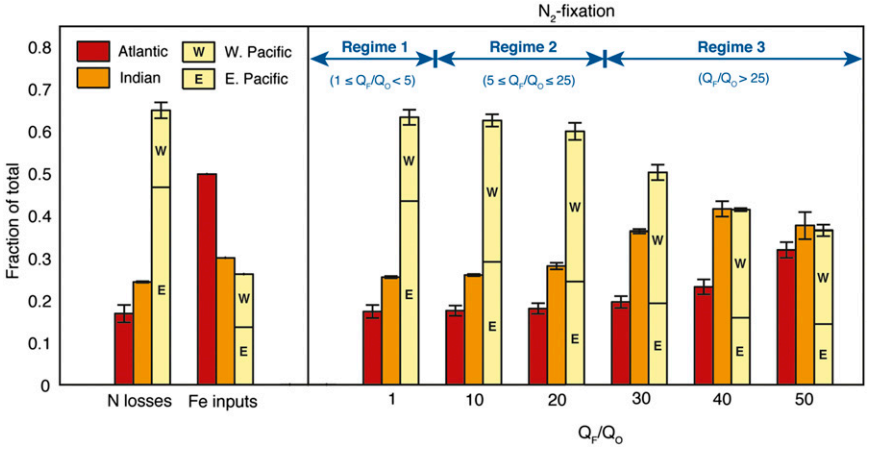

Fig. 1. Distribution of simulated N_2 fixation (*Right*) and its environmental stimuli (*Left*). Basin-integrated rates are given as a fraction of the global total. N losses comprise water column and benthic denitrification, which are prescribed using data-constrained estimates from inverse models (20, 21); Fe inputs to the surface ocean are based on dust deposition rates predicted in an atmospheric model (7). The N_2 fixation distribution varies as diazotroph Fe requirements (Q_F) are raised relative to the fixed Fe requirement of other plankton (Q_O). Bar heights and error bars represent average and SD across four model scenarios with different global rates of benthic denitrification (100, 140, 180, and 220 TgN/y), which bracket the observationally constrained range; The contribution of the Pacific to each process is divided between western and eastern portions, separated along 160°W.

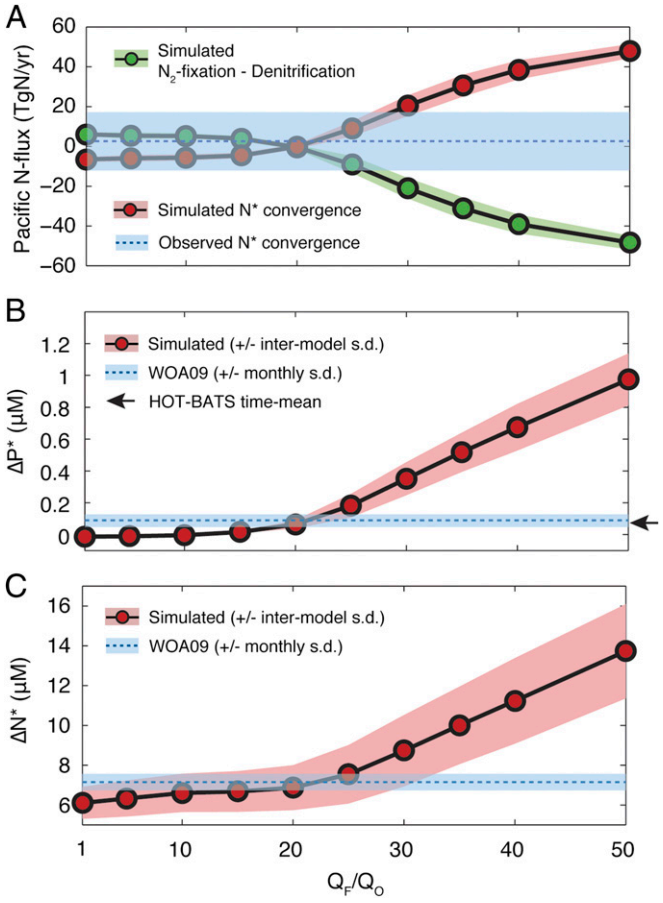

Fig. 2. Geochemical constraints on Fe limitation regime of the modern ocean. Simulated quantities from model Fe limitation scenarios are compared with observations (blue bars). (*A*) N budget of the Pacific Ocean: the basin-scale difference between N_2 fixation and denitrification (green dots) is balanced by a transport convergence of N* into the basin (red dots). Observational constraint applies to transport component, showing mean and SD of 10,000 Monte Carlo calculations of observed N* convergence into the Pacific (Fig. S4). (*B*) Difference in surface P* ($[PO_4^{3-}] - [NO_3^-]/16$) and (*C*) difference in thermocline N* ($[NO_3^-] - 16[PO_4^{3-}]$) between North Pacific and North Atlantic Subtropical Gyres ($\Delta P^* = P^*_{NPSG} - P^*_{NASG}$; $\Delta N^* = N^*_{NASG} - N^*_{NPSG}$). Observed values are computed from World Ocean Atlas 2009 annual mean climatology with error envelopes representing SD between months in the monthly climatology. Arrow on *B* indicates observed P* difference between HOT and BATS locations. In all panels, simulated values and error envelopes represent mean and SD of four benthic denitrification scenarios for each Q_F/Q_O.

reaches agreement with observations in the range $15 < Q_F/Q_O < 25$. Once Fe scarcity precludes complete P* utilization even in the western Pacific (regime 3), it accumulates rapidly in the NPSG and simulated ΔP* diverges sharply from observations. A similar result is obtained when comparing surface P* at the Hawaii Ocean Timeseries (HOT) and Bermuda Atlantic Time Series (BATS) sites, where nutrients have been measured with greater analytical precision for more than two decades. The observed difference between those locations ($P^*_{HOT} - P^*_{BATS}$) of 0.06 ± 0.04 μM is most compatible with regime 2 simulations, with $Q_F/Q_O \sim 20$ (Fig. 2*B*). The interbasin difference in thermocline N* ($\Delta N^* = N^*_{NASG} - N^*_{NPSG}$) exhibits similar behavior to ΔP* as Q_F/Q_O is raised. It increases gradually through regime 2 as N deficits accumulate in the eastern Pacific thermocline, then sharply through regime 3, departing significantly from observations at $Q_F/Q_O > 30$ (Fig. 2*C*).

The stoichiometric differences between Atlantic and Pacific basins, from surface and thermocline waters, therefore point to the intermediate Fe limitation regime (regime 2) as most representative of the modern ocean. While regime 1 appears less likely, it cannot be excluded altogether due to the uncertainty and variability in nutrient observations, and limited spatial and temporal resolution of the physical ocean model we use (19).

The Fe-induced shifts in diazotroph habitat also alter large-scale patterns of organic matter export, and may therefore change the relative size of major suboxic zones undergoing denitrification. In simulations that account for the coupling of O_2 and N cycles, using prognostic rather than prescribed denitrification rates (see *SI Materials and Methods*), the partition of N losses between basins provides an additional constraint on Fe limitation regimes. As Q_F/Q_O is raised, diazotroph communities become increasingly separated from the low-O_2 waters of the eastern Pacific, and eventually relocate toward corresponding waters in the Indian Ocean, where high Fe flux and anoxia coexist (Fig. 1). The accompanying shift in subsurface respiration from the Pacific to Indian Ocean reduces the fraction of global water column denitrification that occurs in the Pacific Ocean (W_{Pac}) from ~90% at $Q_F/Q_O = 1$ to ~40% at $Q_F/Q_O = 50$ (Fig. 3). Under strong Fe limitation, the distribution of N losses as well as inputs should therefore reflect the atmospheric Fe supply, but this is not supported by observations. Consistent with previous constraints, W_{Pac} matches a tracer-based estimate of 75 ± 6% (20) most closely in regime 2 (Fig. 3).

In summary, the intrabasin reorganization of N_2 fixation associated with an intermediate degree of diazotroph Fe limitation (regime 2) brings model predictions into closest agreement with all observational constraints. In contrast, the interbasin shifts accompanying the transition to regime 3, representing strong and widespread Fe limitation, lead to a rapid violation of those constraints. These results are further supported by N isotope distributions (Fig. S6*A*) and the global N inventory (Fig. S6*B*), and are robust against other factors that influence diazotroph growth (Fig. S7) and Fe limitation (Fig. S8).

Within regime 2, the factors limiting local diazotroph growth vary between ocean basins. N_2 fixation is locally limited by PO_4^{3-} throughout most of the Atlantic and Indian oceans, as indicated by low resource limitation factors (γ) for P relative to Fe ($\gamma_{Fe}/\gamma_P > 1$, Fig. 4*A*) (29). In these regions, diazotrophs can obtain sufficient Fe to completely use the excess PO_4^{3-} in upwelling water, either because atmospheric Fe inputs are large or because subsurface P* is scarce due to low NO_3^- removal. In contrast, diazotroph

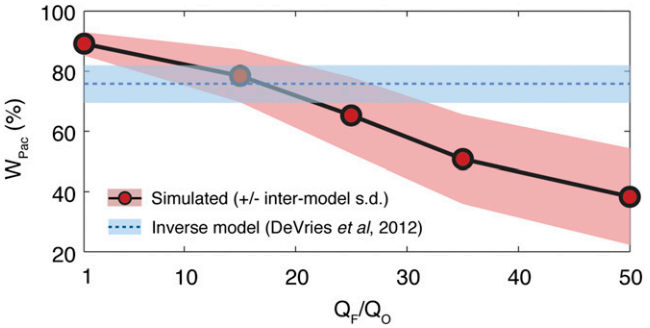

Fig. 3. Additional constraint on Fe limitation regime from model with explicit O_2 cycle. Water-column denitrification is simulated prognostically, and the fraction occurring in the Pacific Ocean (W_{Pac}) declines as Fe limitation of diazotrophs gets stronger. Simulated values represent mean and SD of four simulations with different transport models and dissolved organic matter parameterizations; observational constraint is from an inverse model that optimally matched global data for N deficits, NO_3^- isotope ratios, and excess N_2 gas in subsurface waters (20).

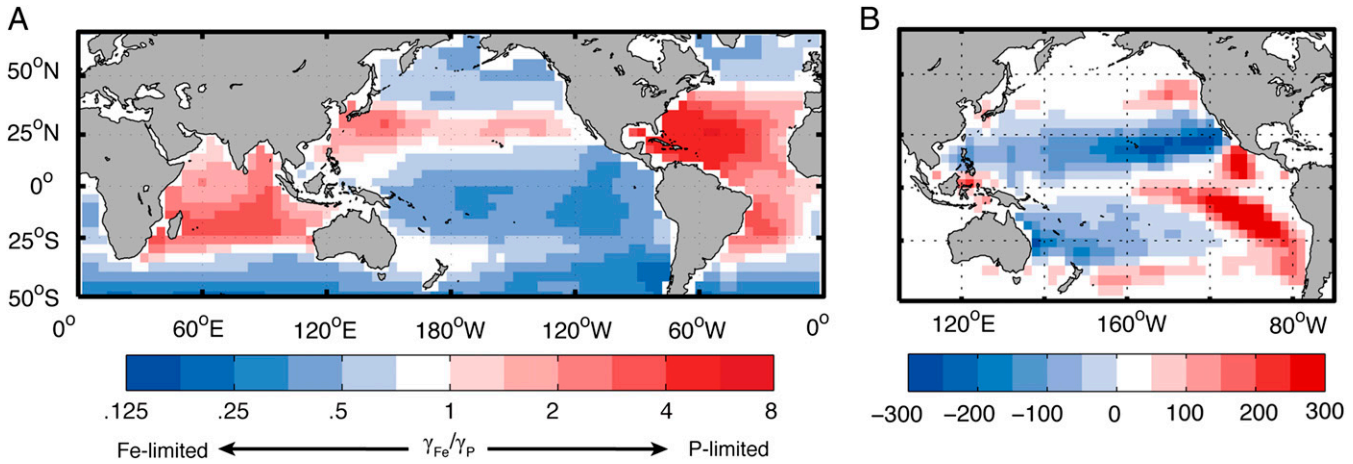

Fig. 4. Local and basin-scale limitation of N_2 fixation rates under modern-ocean conditions ($Q_F/Q_O = 20$). (*A*) Comparison of nutrient limitation factors for model diazotrophs: $\gamma_{Fe} = Fe/(Fe + K_{Fe})$, $\gamma_P = PO_4^{3-}/(PO_4^{3-} + K_P)$, where K_{Fe} and K_P are half-saturation constants for diazotroph growth on Fe and PO_4^{3-}, respectively. Values of γ_{Fe}/γ_P separate regions where diazotrophs are Fe-limited ($\gamma_{Fe}/\gamma_P < 1$) and PO_4^{3-}-limited ($\gamma_{Fe}/\gamma_P > 1$). (*B*) Change in column-integrated N_2 fixation 30 y after the atmospheric Fe supply is raised by 1 g m^{-2} y^{-1} across the Pacific to eliminate Fe limitation. Regions in which N_2 fixation is raised (positive) are almost exactly offset by those where it is lowered (negative), yielding a net increase less than 10 TgN/y (Fig. S9).

communities in much of the low-latitude Pacific Ocean are subject to intensive Fe limitation ($\gamma_{Fe}/\gamma_P < 1$, Fig. 4*A*), and experience P limitation only at the poleward and western margins of the subtropical gyres. Across vast areas of the tropics and eastern subtropics, N_2 fixation is inhibited or excluded in high-PO_4^{3-} surface waters of the Pacific due to Fe scarcity, which results from low dust deposition rates and the upwelling of old waters with a long history of Fe scavenging. In these regions, small-scale Fe additions can promote local diazotroph blooms and enhanced carbon drawdown.

The regulation of N_2 fixation by Fe does not translate to larger spatial scales, however. If limited by Fe inputs rather than N deficits, the integrated fixation rate of the Pacific Ocean could be permanently raised by widespread Fe fertilization, even while N loss rates are held constant. In regime 2, an enhanced basin-wide Fe supply stimulates N_2 fixation in the strongly Fe-limited eastern and equatorial Pacific (Fig. 4*B*), but diazotroph growth along these margins strips excess PO_4^{3-} from waters that flow westward across the basin and feed into the subtropics. Consequently, diazotroph communities that were fueled by downstream PO_4^{3-} transport become starved of this nutrient, suppressing N_2 fixation throughout much of the subtropical gyres (Fig. 4*B*). A few decades after the onset of Fe fertilization, reduced fixation in those downstream environments offsets the regional gains from fertilization (Fig. S9), reaching a new steady state in which basin-integrated N_2 fixation is just 5% greater than its initial rate. Thus, in regime 2, Fe limitation does not prevent diazotrophs from fully compensating the upwelling N deficit in the Pacific Ocean, it simply dictates where within the basin this compensation occurs. The N_2 fixation rate of the whole Pacific is governed by the production of N deficits through denitrification, yielding a close balance between biological sources and sinks of N at the basin scale (Fig. 2*A*).

Taken together, our results reconcile direct observations of Fe limitation of diazotroph growth in the Pacific (30, 31) with geochemical evidence for a spatial coupling of N sources and sinks (6). The key distinction is that Fe limitation operates at the scale of plankton communities and even over larger biogeographical provinces, but does not control the partition of N_2 fixation between ocean basins, which instead reflects the distribution of N loss rates. Although local-scale Fe limitation is confined to the Pacific Ocean in regime 2 of our model (Fig. 4*A* and Fig. S3*B*), it might extend to other ocean basins if systematic differences in Fe sources and utilization exist between basins. Direct observations support regional Fe control of N_2 fixation rates in the Atlantic Ocean (17), potentially indicating a lower

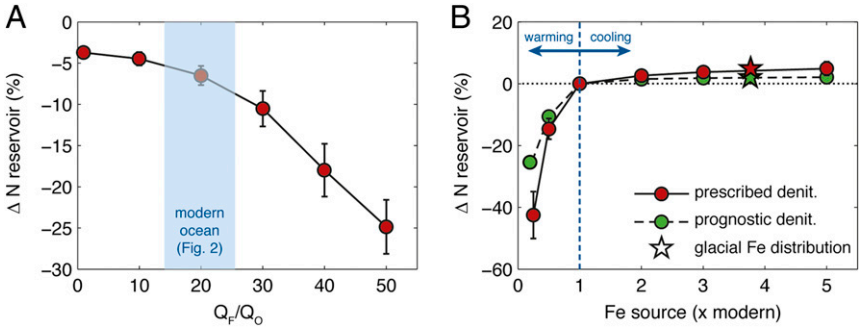

Fig. 5. Sensitivity of the ocean N reservoir to climate forcing. (*A*) Change in steady-state N reservoir following a prescribed doubling of global water-column denitrification (denit), as a function of diazotroph Fe limitation regimes. Blue band indicates the range of Q_F/Q_O allowed by modern-ocean constraints (Fig. 2). (*B*) Change in N reservoir induced by altering Fe inputs to the ocean for $Q_F/Q_O = 20$, in models with prescribed and prognostic denitrification rates. Glacial simulations use dust deposition fluxes predicted for the Last Glacial Maximum (7); others scale the modern distribution by a constant factor. For cases with prescribed denitrification in *A* and *B*, the mean and SD of four simulations with differing benthic denitrification rates are given.

solubility of windblown dust in that basin, or a higher Fe requirement of its dominant diazotroph group *Trichodesmium sp.*, relative to the unicellular groups that dominate the Pacific (12, 32).

The existence of strong negative feedbacks that regulate the N reservoir has been assumed to require a very close proximity of diazotroph habitats to N removal sites. We tested this assumption by simulating the response of N_2 fixation to the climatically forced variations of water-column denitrification inferred over both glacial and modern periods (33, 34). Within the intermediate regime of Fe control implied by observational constraints, an instantaneous doubling of denitrification in suboxic zones is counteracted fast enough by N_2 fixation to limit oceanic N loss to <10% of its current reservoir, before a new steady state is reached (Fig. 5*A*). Basin-scale coupling of N sources and sinks is sufficient to produce a strong stabilizing feedback, because new N deficits generated by enhanced denitrification in the Pacific are transported only through shallow circulation pathways, and compensated rapidly by N_2 fixation within the basin. To weaken this feedback, N deficits generated in the Pacific must penetrate the deeper ocean and traverse sluggish circulation pathways, before they are compensated in the dustier Atlantic and Indian oceans. This occurs only in the strong Fe limitation regime, well outside the plausible range of tracer constraints (Fig. 5*A*). In contrast to previous hypotheses and model predictions (9, 35), our results therefore indicate that Fe scarcity cannot decouple N_2 fixation from denitrification over the timescales required to significantly perturb the N reservoir, under modern Fe supply rates.

We also tested the hypothesis that global N_2 fixation is subject to climate-forced variations mediated by the Fe supply, in which enhanced dust fluxes associated with climate cooling are argued to stimulate N inputs to the ocean (4, 10). However, because basin-scale N_2 fixation rates are not limited by Fe under contemporary conditions (Fig. 4*B*), Fe additions have limited potential to change the oceanic N inventory. Raising global Fe inputs to the ocean by up to five times the modern rate allows for no more than a 5% increase in our model's N reservoir (Fig. 5*B*), even with the altered dust distribution inferred for the last glacial maximum (7). However, the N reservoir's stability under dustier climate regimes is in stark contrast to its behavior when dust deposition is reduced. As the Fe supply falls below its modern rate, the Pacific Ocean is soon unable to support enough N_2 fixation to balance its N losses, resulting in a sustained imbalance of the N budget that persists until N deficits are exported and compensated in other basins. This mechanism results in substantial global N loss before a new steady state is reached. When atmospheric Fe sources are lowered to 25% of modern values, over 40% of oceanic fixed N is lost and export production is reduced by a corresponding factor. A slightly weaker perturbation is found in simulations with prognostic denitrification, in which Pacific N loss rates decline in response to decreasing export, but the ocean still loses >25% of its N reservoir (Fig. 5*B*). These results raise the possibility that reduced dust fluxes predicted under a warming climate (7) could suppress marine N_2 fixation and weaken the biological carbon pump.

Materials and Methods

Biogeochemical cycles of N, P, and Fe were simulated in a coarse-resolution Ocean General Circulation Model (4° × 4°, 24 vertical layers), in which flow fields are optimized to satisfy dynamical balances and match hydrographic tracers (19). Elemental fluxes are coupled through a simple ecosystem model (18) comprising diazotropic plankton (*F*) and other nonfixing plankton (*O*) with growth and mortality governed by:

$$\frac{dO}{dt} = \mu_o \min\left(\frac{P}{P+K_P}, \frac{N}{N+K_N}, \frac{Fe}{Fe+K_{Fe}}\right) O - MO \quad [1]$$

$$\frac{dF}{dt} = \mu_F \min\left(\frac{P}{P+K_P}, \frac{Fe}{Fe+K_{Fe}}\right) F - MF, \quad [2]$$

where μ_o and μ_F represent temperature and light-dependent maximum growth rates, K_X is the half-saturation concentration for growth on element *X*, and *M* represents mortality and includes a quadratic term to represent grazing by zooplankton. Diazotrophs can grow independent of N but are handicapped by slower growth rates ($\mu_F < \mu_o$) and a higher Fe requirement that is manipulated between simulations to vary the strength of Fe limitation they experience. Fe is added to the surface ocean by atmospheric dust deposition, undergoes complexation with organic ligands, and is removed by scavenging onto organic particles (22). All simulations were integrated to a steady state in which model N and Fe budgets reach close balance, generally requiring 5–10 thousand years.

We compared simulated and observed geochemical quantities, which integrate the signature of N_2 fixation over time and space scales much longer than biological rate measurements, and are relatively insensitive to poorly constrained model parameters. An observational constraint was placed on the biological N budget (N_2 fixation minus denitrification) of the Pacific Ocean, by computing the balancing physical transport of observed N* across the basin's boundaries. Uncertainties in the nutrient data and transport velocities were propagated into this estimate by adding random samples from the observed variance of N* and randomly selecting between different circulation models in 10,000 Monte Carlo iterations. Stoichiometric tracers (surface P* and thermocline N*) were averaged across the North Pacific and North Atlantic subtropical gyres, and the differences between basins were computed. These large-scale differences provide more robust constraints than mean tracer values for individual basins, because they are not sensitive to variations in the oceanic N reservoir between simulations. A second model configuration was used to predict the interbasin partition of suboxic waters under each Fe limitation scenario in a higher resolution. This incorporated a prognostic O_2 cycle and increased model resolution to 2° × 2° to better resolve low oxygen zones. When oxygen becomes fully depleted, organic matter remineralization proceeds through denitrification, consuming 6.5 moles of NO_3^- per mole remineralized.

See *SI Materials and Methods* for more detailed description of model simulations and observational constraints.

ACKNOWLEDGMENTS. We thank Tim DeVries for supplying transport models and assisting with methods. This work was supported by a NASA Earth Systems Science Fellowship (to T.W.) and grants from the Gordon and Betty Moore Foundation and National Science Foundation (to C.D.).

1. Karl D, et al. (2002) Dinitrogen fixation in the world's oceans. *Biogeochemistry* 57/58(1):47–98.
2. Redfield AC, Ketchum BH, Richards FA (1963) The influence of organisms on the composition of seawater. *The Sea*, ed Hill MN (Interscience, New York), Vol 2, pp 26–77.
3. Tyrrell T (1999) The relative influences of nitrogen and phosphorus on oceanic primary production. *Nature* 400(6744):525–531.
4. Falkowski PG (1997) Evolution of the nitrogen cycle and its influence on the biological sequestration of CO_2 in the ocean. *Nature* 387(6630):272–275.
5. Deutsch C, Weber T (2012) Nutrient ratios as a tracer and driver of ocean biogeochemistry. *Annu Rev Mar Sci* 4(1):113–141.
6. Deutsch C, Sarmiento JL, Sigman DM, Gruber N, Dunne JP (2007) Spatial coupling of nitrogen inputs and losses in the ocean. *Nature* 445(7124):163–167.
7. Mahowald NM, et al. (2006) Change in atmospheric mineral aerosols in response to climate: Last glacial period, preindustrial, modern, and doubled carbon dioxide climates. *J Geophys Res* 111(D10):D10202, 10.1029/2005JD006653.
8. Monteiro FM, Dutkiewicz S, Follows MJ (2011) Biogeographical controls on the marine nitrogen fixers. *Global Biogeochem Cycles* 25(2):GB2003, 10.1029/2010GB003902.
9. Moore CM, et al. (2009) Large-scale distribution of Atlantic nitrogen fixation controlled by iron availability. *Nat Geosci* 2(12):867–871.
10. Broecker WS, Henderson GM (1998) The sequence of events surrounding Termination II and their implications for the cause of glacial-interglacial CO_2 changes. *Paleoceanography* 13(4):352–364.
11. Eugster O, Gruber N, Deutsch C, Jaccard SL, Payne MR (2013) The dynamics of the marine nitrogen cycle across the last deglaciation. *Paleoceanography* 28(1):116–129.
12. Capone DG, et al. (2005) Nitrogen fixation by Trichodesmium spp.: An important source of new nitrogen to the tropical and subtropical North Atlantic Ocean. *Global Biogeochem Cycles* 19(2):GB2024, 10.1029/2004GB002331.
13. Gruber N, Sarmiento JL (1997) Global patterns of marine nitrogen fixation and denitrification. *Global Biogeochem Cycles* 11(2):235–266.
14. Großkopf T, et al. (2012) Doubling of marine dinitrogen-fixation rates based on direct measurements. *Nature* 488(7411):361–364.

15. Montoya JP, et al. (2004) High rates of N_2 fixation by unicellular diazotrophs in the oligotrophic Pacific Ocean. *Nature* 430(7003):1027–1032.
16. Zehr JP, et al. (2001) Unicellular cyanobacteria fix N_2 in the subtropical North Pacific Ocean. *Nature* 412(6847):635–638.
17. Luo YW, Lima ID, Karl DM, Doney SC (2013) Data-based assessment of environmental controls on global marine nitrogen fixation. *Biogeosciences Discuss* 10(4):7367–7412.
18. Weber T, Deutsch C (2012) Oceanic nitrogen reservoir regulated by plankton diversity and ocean circulation. *Nature* 489(7416):419–422.
19. DeVries T, Primeau F (2011) Dynamically and observationally constrained estimates of water-mass distributions and ages in the global ocean. *J Phys Oceanogr* 41(12): 2381–2401.
20. DeVries T, Deutsch C, Primeau F, Chang B, Devol A (2012) Global rates of water-column denitrification derived from nitrogen gas measurements. *Nat Geosci* 5(8): 547–550.
21. DeVries T, Deutsch C, Rafter PA, Primeau F (2012) Marine denitrification rates determined from a global 3-dimensional inverse model. *Biogeosciences Discuss* 9(10): 14013–14052.
22. Parekh P, Follows MJ, Boyle EA (2005) Decoupling of iron and phosphate in the global ocean. *Global Biogeochem Cycles* 19(2):GB2020, 10.1029/2004GB002280.
23. LaRoche J, Breitbarth E (2005) Importance of the diazotrophs as a source of new nitrogen in the ocean. *J Sea Res* 53(1-2):67–91.
24. Kustka A, Sanudo-Wilhelmy S, Carpenter EJ, Capone DG, Raven JA (2003) A revised estimate of the iron use efficiency of nitrogen fixation, with special reference to the marine cyanobacterium *Trichodesmium* spp. (Cyanophyta). *J Phycol* 39(1):12–25.
25. Berman-Frank I, Cullen JT, Shaked Y, Sherrell RM, Falkowski PG (2001) Iron availability, cellular iron quotas, and nitrogen fixation in *Trichodesmium*. *Limnol Oceanogr* 46(6):1249–1260.
26. Deutsch C, Gruber N, Key RM, Sarmiento JL, Ganaschaud A (2001) Denitrification and N_2 fixation in the Pacific Ocean. *Global Biogeochem Cycles* 15(2):483–506.
27. Letelier RM, Karl DM (1998) *Trichodesmium* spp. physiology and nutrient fluxes in the North Pacific subtropical gyre. *Aquat Microb Ecol* 15(3):265–276.
28. Garcia H, Locarnini R, Boyer T, Antonov J (2010) *World Ocean Atlas 2009: Nutrients (Phosphate, Nitrate, Silicate), (NOAA Atlas NESDIS*) (US Gov. Print. Off, Washington, DC), Vol 4.
29. Sañudo-Wilhelmy SA, et al. (2001) Phosphorus limitation of nitrogen fixation by *Trichodesmium* in the central Atlantic Ocean. *Nature* 411(6833):66–69.
30. Chappell PD, Moffett JW, Hynes AM, Webb EA (2012) Molecular evidence of iron limitation and availability in the global diazotroph *Trichodesmium*. *ISME J* 6(9): 1728–1739.
31. Bonnet S, et al. (2008) Nutrient limitation of primary productivity in the Southeast Pacific (BIOSOPE cruise). *Biogeosciences* 5(1):215–225.
32. Moisander PH, et al. (2010) Unicellular cyanobacterial distributions broaden the oceanic N_2 fixation domain. *Science* 327(5972):1512–1514.
33. Deutsch C, Brix H, Ito T, Frenzel H, Thompson L (2011) Climate-forced variability of ocean hypoxia. *Science* 333(6040):336–339.
34. Altabet MA, Francois R, Murray DW, Prell WL (1995) Climate-related variations in denitrification in the Arabian Sea from sediment $^{15}N/^{14}N$ ratios. *Nature* 373(6514): 506–509.
35. Moore JK, Doney SC (2007) Iron availability limits the ocean nitrogen inventory stabilizing feedbacks between marine denitrification and nitrogen fixation. *Global Biogeochem Cycles* 21(2):GB2001, 10.1029/2006GB002762.
36. Middelburg JJ, Soetaert K, Herman PMJ, Heip CHR (1996) Denitrification in marine sediments: A model study. *Global Biogeochem Cycles* 10(4):661–673.